RADIATION OF AN ELASTIC WAVE DURING AN EXPLOSION IN A VARIABLY COMPRESSED POROUS MEDIUM

A. A. Zverev, E. E. Lovetskii, and V. S. Fetisov

UDC 534.222.2

The question of the radiation of an elastic wave in a camouflet explosion was considered in several papers [1-3]. Most detailed computations are presented in [3], where the problem of expansion of the gas cavity in an elastic—plastic dilating medium was investigated. It was assumed in [3] that a constant irreversible compression of the medium occurs on the destruction wave front. Such an approximation does not permit taking account of the reverse influence of the emitted elastic wave on the destruction wave parameters in the case of not too high compressions.

The parameters of an elastic wave emitted in a camouflet explosion are computed in this paper for the case when substance compression on the destruction wave front is variable.

The source of medium motion is a gas in a cavity whose radius is a_0 at the initial instant. The gas pressure at this time is p_0. For $t > 0$ a spherical shock starts to be propagated from the cavity. Initially, the velocity of shock propagation exceeds the velocity of the longitudinal waves in the medium. Instantaneous compression of the medium occurs on the wave front because of selection. We will characterize the degree of compression of the medium on the front by the compression $\varepsilon(R) = 1 - \rho_0/\rho(R)$, where R is the radius of the shock front, ρ_0 is the initial density of the medium, and $\rho(R)$ is the density achievable at the front. It is assumed that destruction of the medium occurs right after the compression. Plastic flow of the medium occurs behind the shock front that coincides with the destruction wave front, and this flow is accompanied by a change in density because of the effect of dilatancy [3-5]. Compressibility of the pieces of the shattered medium is not taken into account here. Let us note that such a pattern for the description of cavity expansion and shock front motion can be utilized just while the front velocity exceeds the velocity of longitudinal wave propagation. In this stage the motion of the medium is described by the motion and continuity equations and by the equation of the dilatation change in volume

$$\frac{\partial u}{\partial t} + u\frac{\partial u}{\partial r} = \frac{1}{\rho}\frac{\partial \sigma_r}{\partial r} + \frac{2}{\rho}\frac{\sigma_r - \sigma_\varphi}{r}, \qquad (1)$$

$$\frac{\partial \rho}{\partial t} + \frac{1}{r^2}\frac{\partial}{\partial r}(r^2\rho u) = 0,$$

$$\frac{\partial u}{\partial r} + 2\frac{u}{r} = \Lambda\left|\frac{\partial u}{\partial r} - \frac{u}{r}\right|,$$

where u is the mass flow rate of the medium; ρ, density; σ_r and σ_φ, radial and azimuthal components of the stress tensor; and Λ, rate of dilatancy which we shall consider constant. It is assumed that the Prandtl plasticity condition

$$\sigma_r - \sigma_\varphi = k + m(\sigma_r + 2\sigma_\varphi),$$

is satisfied behind the wave front, where k and m are the adhesion and friction coefficients, respectively. The conditions of mass and momentum conservation

$$u(R) = \varepsilon(R)\dot{R},$$

$$\sigma_r(R) = -\rho_0\varepsilon(R)\dot{R}^2 - \sigma^*,$$

are satisfied behind the wave front (the destruction wave), where $\dot{R}$ is the velocity of the destruction wave front and σ^* is the crushing strength.

The condition for adiabatic expansion of explosive gases yields the boundary condition on the cavity wall

Moscow. Translated from Zhurnal Prikladnoi Mekhaniki i Tekhnicheskoi Fiziki, No. 6, pp. 47-52, November-December, 1983. Original article submitted October 11, 1982.

0021-8944/83/2406-0807$07.50

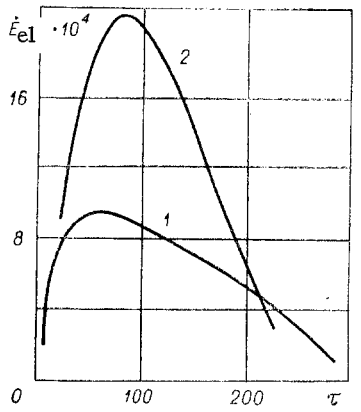

Fig. 1

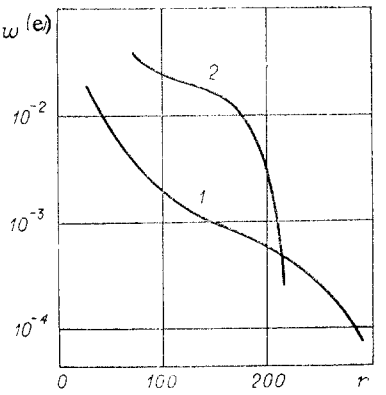

Fig. 2

$$\sigma_r(a) = -p_0(a_0/a)^{3\gamma},$$

where a is the running radius of the cavity and γ is the adiabatic index.

We take the expression

$$\varepsilon(R) = \varepsilon_0(a_0/R)^{\lambda} \quad (\lambda > 0).$$

for the dependence $\varepsilon(R)$. Furthermore, the camouflet equation, similar to the equation in [5], can be obtained by a standard method, and appears as follows in dimensionless form:

$$\frac{dy}{dx} + N(x)\,y = M(x), \quad y = \dot{x}^2, \quad \ddot{x} = \frac{1}{2}\frac{\partial y}{\partial x}, \tag{2}$$

$$M(x) = 2\frac{(Z^{\alpha} - x^{\alpha})\frac{k}{3mp_0} - x^{\alpha}\Sigma_r(x) - Z^{\alpha}\sigma^*/p_0}{x^{n}Y},$$

$$N(x) = \frac{2n}{x} - 2\frac{x^{n}[nX - \varepsilon(Z)\,Z^{\alpha-2(n-\lambda)}]}{Y},$$

$$X = \int_1^Z r_0^2 r^{\alpha-3-2n}(r_0)\,dr_0, \quad Y = \int_1^Z r_0^2 r^{\alpha-2-n}(r_0)\,dr_0,$$

$$\alpha = 6m/(2m+1), \quad n = (2-\Lambda)/(1+\Lambda), \quad x = a/a_0, \quad Z = R/a_0, \quad \Sigma_r = \sigma_r/p_0.$$

Here $r(r_0)$ is the dependence of the Eulerian on the Lagrangian coordinate, which is determined from the equations

$$\frac{r}{r_0} = \frac{1}{\rho}\left(\frac{r_0}{r}\right)^2, \quad \rho(r) = \frac{1}{1-\varepsilon_0 r_0^{-\lambda}}\left(\frac{r_0}{r}\right)^{2-n}.$$

The r and r_0 in (2) are dimensionless and expressed in units of a_0, while ρ is expressed in units of ρ_0, and the dot denotes differentiation with respect to the dimensionless time $\tau = t\sqrt{p_0/\rho_0}/a_0$. The initial condition of (2) has the form $y(x = 1) = \varepsilon_0$. Solving (2), a complete description can be obtained of the motion of the cavity, the destruction wave front, the medium between the cavity and the destruction wave front within the framework of the model formulated. This solution will be valid until the front velocity exceeds the velocity of longitudinal wave propagation in this medium. The quantity $\dot{R}$ diminishes with time and at a certain time $t = t^*$ the destruction wave front velocity $\dot{R}$ is compared to the velocity of longitudinal wave propagation. At this time an elastic wave that is propagated at the velocity c_l (c_l is the longitudinal speed of sound in the medium) starts to be emitted from the destruction wave front. The physical quantities in the elastic domain are expressed in terms of the potential of elastic displacements $f(\Delta)$, $\Delta = c_l t/a_0 - r/a_0$:

$$\sigma_r^{(e)} = -\rho_0 c_l^2\left[\frac{\ddot{f}}{r} + 2\frac{1-2\nu}{1-\nu}\left(\frac{\dot{f}}{r^2} + \frac{f}{r^3}\right)\right] - p_h,$$

$$\sigma_{\varphi}^{(e)} = -\rho_0 c_l^2\left[\frac{\ddot{f}}{r}\frac{\nu}{1-\nu} - \frac{1-2\nu}{1-\nu}\left(\frac{\dot{f}}{r^2} + \frac{f}{r^3}\right)\right] - p_h,$$

$$v^{(e)} = c_l\left(\frac{\ddot{f}}{r} + \frac{\dot{f}}{r^2}\right), \quad w^{(e)} = a_0\left(\frac{\dot{f}}{r} + \frac{t}{r^2}\right), \quad \rho^{(e)} = \rho_0\left(1 + \frac{\ddot{f}}{r}\right),$$

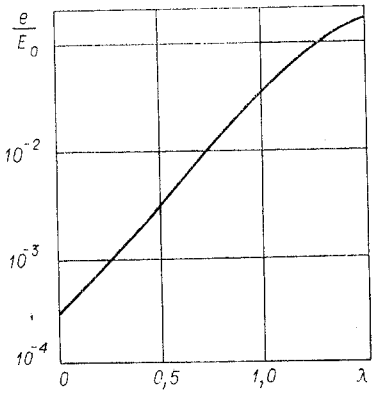

Fig. 3

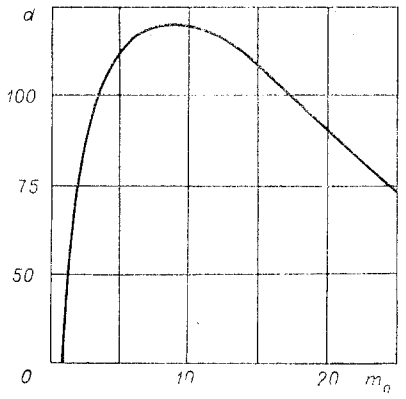

Fig. 4

where p_h is the background pressure, $w^{(e)}$ is the displacement, $v^{(e)}$ is the mass flow rate of the medium, and ν is the Poisson ratio; the superscript (e) means that the corresponding quantities are taken in the elastic zone.

Taking account of the elastic wave, the conditions on the destruction wave front become

$$u(R) = \dot{R}\varepsilon(R) + v^{(e)}(R)[1 - \varepsilon(R)],$$

$$\sigma_r(R) = \sigma_r^{(e)}(R) - \rho^{(e)}(R)\,\varepsilon(R)[\dot{R} - v^{(e)}(R)].$$

As before, we take the condition of destruction by crushing on the destruction wave front:

$$\sigma_r^{(e)}(R) = -\sigma^*. \tag{3}$$

which results in the equation for $f(\Delta)$:

$$\frac{\ddot{f}}{R} = \frac{\sigma^* - p_h}{\rho_0 c_l^2} - 2\,\frac{1-2\nu}{1-\nu}\left[\frac{\dot{f}}{R^2} + \frac{f}{R^3}\right]. \tag{4}$$

We now turn to Lagrange variables in (1) which describes the plastic flow of the destroyed medium. The third equation of the system (1) yields

$$u = c(t)/r^n, \quad n = (2 - \Lambda)/(1 + \Lambda).$$

The boundary conditions for r = R yield for c(t)

$$c = R^n[\dot{R}\varepsilon + (1 - \varepsilon)v^{(y)}(R)]. \tag{5}$$

Then, substituting the expression for u into the first equation in the system (1), we obtain the camouflet equation valid for t > t* after appropriate manipulations:

$$A\ddot{Z} + B\dot{Z}^2 + C\dot{Z} = D, \tag{6}$$

$$A = \varepsilon(Z)Y, \quad c_0 = \sqrt{p_0/\rho_0},$$

$$B = \left(\frac{n}{Z}\,\varepsilon + \frac{\partial\varepsilon}{\partial Z}\right)Y - nZ^n\varepsilon^2 X + Z^{\alpha-n}\,\frac{\rho^{(y)}(Z)}{\rho_0}\,\varepsilon,$$

$$C = \left[\frac{n}{Z}(1-\varepsilon)\,\frac{v^{(y)}}{c_0} - \frac{v^{(y)}}{c_0}\,\frac{\partial\varepsilon}{\partial Z} + 3(1-\varepsilon)\,\frac{c_l}{c_0}\,\frac{f}{Z^4}\right]Y - 2\varepsilon(1-\varepsilon)\,nZ^n\,\frac{v^{(e)}}{c_0}\,X - 2\varepsilon\,\frac{v^{(e)}}{c_0}\,Z^{\alpha-n},$$

$$D = \frac{Z^\alpha - x^\alpha}{Z^n}\,\frac{k}{3mp_0} - \frac{x^\alpha}{Z^n}\,\Sigma_r(x) - Z^{\alpha-n}\,\frac{\sigma^*}{p_0} + (1-\varepsilon)\,\frac{c_l}{c_0}\,\frac{\dot{f}}{Z^3}\,Y.$$

The joint propagation of the destruction and the elastic wave is described completely by (4) and (6). Values of the appropriate quantities at t = t* are used as initial values for the solution of (4) and (6). Let us note that for constant compression on the destruction wave front $\varepsilon(R) = \varepsilon_0 = \text{const}$, neglecting the second term in the square brackets in (5) we obtain the equation presented in [3]. This latter neglect is valid only under the con-

dition $\dot{R}\varepsilon >> v^{(e)}$, which is not satisfied if the quantity ε is sufficiently small. The smallness of ε means that the condition $\varepsilon >> \sigma^*/\rho c_l^2$ for which the equations presented in [3] are valid is not satisfied.

Therefore, the equations obtained above describe the development of a camouflet explosion and afford an opportunity to determine the characteristics of the elastic wave emitted from the destruction wave front. Equations (2), (4), and (6) can be solved only by using numerical methods. We turn to the results of numerical computations.

Several modifications were computed during solution of the problem. In all the modifications the computation was for $p_0 = 7 \cdot 10^4$ MPa, $a_0 = 3$ m, $\gamma = 1.4$, $k = -1$ MPa, $m = 0.1$, $\Lambda = 0.07$, $\sigma^* = 50$ MPa, $\nu = 0.33$, $c_l = 5000$ m/sec, and $\rho_0 = 2.8$ g/cm^3.

Graphs of the time dependence of the dimensionless quantity $\dot{E}_{el}$ are shown in Fig. 1, where

$$\dot{E}_{el} = 4\pi R^2 \sigma^* v^{(\gamma)}(R),$$

Here E_{el} determines the quantity of energy emitted from the destruction wave front. This energy later goes partially into the formation of residual elastic displacements of the medium, i.e., goes over into energy of residual elastic strain. The other part goes over into the seismic wave energy and goes to infinity. The initial compression for curves 1 and 2 is $\varepsilon_0 = 0.05$. Curve 1 corresponds to constant compression at the destruction wave front ($\lambda = 0$), and 2 to variable compression ($\lambda = 1$). It should be taken into account that real values of $\dot{E}_{el}$ are an order of magnitude higher for curve 2 than is presented in Fig. 1. It is seen from Fig. 1 that in the case of variable compression the rate of energy emission from the destruction wave front into the elastic domain exceeds by more than an order the rate of emission for the case $\lambda = 0$. Consequently, the energy emitted from the front into the elastic domain for $\lambda = 1$ also substantially exceeds the analogous quantity for $\lambda = 0$. This result is related to the fact that energy dissipation for $\lambda = 1$, which is related to closing of the pores on the destruction wave front, diminishes as compared to the case $\lambda = 0$. This results in an increase in the size of the destruction zone (at identical times), and therefore, to an increase in E_{el}. For $\lambda = 1$ E_{el} is 26% of the explosion energy while for $\lambda = 0$ this quantity is 2.5%. The increase in E_{el} in the case of variable compression results in a substantial increase in the elastic strains.

The spatial profile of the deformations in the elastic wave is represented in Fig. 2. Curve 1 — $\lambda = 0$, $\varepsilon_0 = 0.05$, curve 2 — $\lambda = 1$, $\varepsilon_0 = 0.05$. The curves are presented at times corresponding to the halt of the destruction wave front.

The question of the magnitude of the elastic energy emitted at infinity is of primary value for the seismology of an underground explosion. This energy was computed analogously to [3]. A graph of the dependence of the energy emitted at infinity on the compression index λ (E_0 is the explosion energy) is given in Fig. 3. As λ increases from 0 to 1 the quantity e grows by two orders. Such a growth of the emitted elastic energy is confirmed by the following estimate. The elastic energy is proportional to $4\pi R^2 \sigma_r^{(e)}(R) w^{(e)}(R) \sim R^2 \sigma^* R \sigma^*/E \sim R^3$, where E is Young's modulus, and R is the characteristic radius of the elastic wave emitter. Substitution of the elastic radii from the different computation modifications yields the same order of energy growth with the rise in λ. Therefore, the results of the computation show that taking account of the variability of the compression on the destruction wave front results in a substantial increase in both the total elastic energy, and the energy that goes off to infinity.

The dependence of the quantity $d = e(\lambda = 1)/e(\lambda = 0)$, i.e., the ratio of the energies emitted at infinity for $\lambda = 1$ to the same energy computed for $\lambda = 0$ on the initial compression is represented in Fig. 4. It is seen that for a medium with ε_0 of the order of 10% (but ε_0 agrees with the initial porosity of the medium) the effect of an increase in e is most substantial.

The consideration presented in this paper shows that taking account of the variability of the compression of the medium on the destruction wave front yields a substantial change in the elastic signal characteristics of a camouflet explosion.

The authors are grateful to O. V. Nagornov for useful remarks and discussion.

LITERATURE CITED

1. M. A. Sadovskii (ed.), Mechanical Effect of an Underground Explosion [in Russian], Nedra, Moscow (1971).
2. A. B. Bagdasaryan, "Analysis of the effect of an explosion in brittle mountain rock (destruction by crushing, formation of spall cracks and rupture)," Zh. Prikl. Mekh. Tekh. Fiz., No. 5 (1970).
3. S. Z. Dunin, O. V. Nagornov, and E. A. Popov, "Elastic wave emission in a camouflet explosion," Izv. Akad. Nauk SSSR, Fiz. Zemli, No. 2 (1982).
4. V. N. Nikolaevskii, K. S. Basniev, A. G. Gorbunov, and G. A. Zotov, Mechanics of Saturated Porous Media [in Russian], Nedra, Moscow (1970).
5. S. Z. Dunin and V. K. Sirotkin, "Expansion of a gas cavity in brittle rock with the dilatancy properties of the soil taken into account," Zh. Prikl. Mekh. Tekh. Fiz., No. 4 (1977).

BLAST WAVES IN FROZEN SOILS

G. M. Lyakhov and G. B. Frash

UDC 624.131+551.345

We present results of experimental studies of spherical blast waves in seasonally frozen soils with different physical and mechanical properties at different temperatures. A comparison with results in [1, 2] shows that the wave parameters depend strongly on the characteristics of the soil in the initial unfrozen state and on the temperature. When the temperature falls, the maximum stresses and the wave velocity increase, but the duration of the wave decreases. The general character of the extinction and flattening of waves in frozen soils, just as in unfrozen soils, is typical of media having plastic properties and bulk viscosity [2].

1. Characteristics of Soils and Test Conditions. Frozen soils are four-component media containing solid mineral particles forming the skeleton, unfrozen water, ice, and air. We denote the volume fractions of the components as follows: air (free interstitial space), α_1; water, α_2; mineral particles, α_3; ice, α_4 (α_4 is also called the volumetric iciness); ρ_1, ρ_2, ρ_3, ρ_4 are the densities of the corresponding components. These quantities are related to the density of the soil ρ_0, the mass (weight) moisture content w, and the gravimetric iciness i by the equations

$$\alpha_1 + \alpha_2 + \alpha_3 + \alpha_4 = 1, \quad \alpha_1\rho_1 + \alpha_2\rho_2 + \alpha_3\rho_3 + \alpha_4\rho_4 = \rho_0,$$
$$\alpha_4\rho_4/(\alpha_2\rho_2 + \alpha_4\rho_4) = i, \quad (\alpha_2\rho_2 + \alpha_4\rho_4)/\alpha_3\rho_3 = w. \tag{1.1}$$

When the temperature falls the volume contents of the components change. This occurs as a result of possible migration of water from the lower layers of the soil to the frost front, and also as a result of the gradual freezing of the interstitial water [3, 4]. Therefore, the values of the quantities listed above must correspond to the temperature at which the experiments are performed and also to the initial (atmospheric) pressure.

The experiments were performed in sandy and loamy soils of natural structure under conditions of seasonal freezing to a depth of 0.45-0.5 m. The granulometric composition of the sandy soil is shown in Table 1.

At a soil temperature t = −0.2°C the average values of the soil characteristics were: ρ_0 = 1840 kg/m^3, ρ_3 = 2660 kg/m^3, w = 0.27, i = 0.73.

The granulometric composition of the loamy soil is shown in Table 2.

In granulometric composition the soil falls into the category of loam, close to sandy loam. At temperatures −0.2°C and −0.4°C the average values of the characteristics of the components were: ρ_0 = 1920 kg/m^3; ρ_3 = 2680 kg/m^3; w = 0.22 in both cases; and i = 0.5 and 0.75, respectively.

Moscow. Translated from Zhurnal Prikladnoi Mekhaniki i Tekhnicheskoi Fiziki, No. 6, pp. 52-57, November-December, 1983. Original article submitted October 26, 1982.

0021-8944/83/2406-0811$07.50